Dalton Transactions

Accepted Manuscript

ROYAL SOCIETY OF CHEMISTRY

www.rsc.org/dalton

Cite this: DOI: 10.1039/c0xx00000x

www.rsc.org/xxxxxx

ARTICLE TYPE

2-(1-Aryliminoethyl)-9-arylimino-5,6,7,8-tetrahydrocycloheptapyridyl iron(II) dichloride: Synthesis, characterization, and the highly active and tunable active species in ethylene polymerization

Fang Huang,[a,b] Qifeng Xing,[b] Tongling Liang,[b] Zygmunt Flisak,[b,c] Bin Ye, [a,b] Xinquan Hu, [*a] Wenhong Yang, [b] Wen-Hua Sun [*b]

Received (in XXX, XXX) Xth XXXXXXXXX 20XX, Accepted Xth XXXXXXXXX 20XX
DOI: 10.1039/b000000x

Abstract: A series of 2-(1-arylimino)ethyl-9-arylimino-5,6,7,8-tetrahydrocycloheptapyridine derivatives was synthesized and fully characterized, and thereafter reacted with iron dichloride to form their corresponding iron(II) complexes. The single crystals of representative organic and iron complex compounds were obtained and figured out by the X-ray diffraction analysis, indicating the distorted bipyramidal geometry around the core iron. Moreover, DFT calculations were performed on selected species to determine their structural features. On treatment with either MAO or MMAO, all iron complex pre-catalysts performed high activities (up to 1.56 × 10^7 gPE·mol^{-1}(Fe)·h^{-1}) toward ethylene polymerization. Regarding nature of the ligands and reaction parameters, their catalytic activities have been carefully investigated as well as the characters of obtained polyethylenes. The ring strain of the fused-cycloheptane of the ligands within iron complexes was considered in affecting their catalytic performance in ethylene polymerization. The active species were activated and controlled by using co-catalyst of better MMAO than MAO, and the obtained polyethylenes with MMAO showed relatively narrower molecular polydispersity than correspondent polyethylenes with MAO.

Introduction

In past two decades, we have witnessed the rapid developments of late-transition metal complexes as pre-catalysts in ethylene reactivity;[1] which was initiated through discovering the highly active pre-catalysts of the α-diiminometal (Ni^{2+} or Pd^{2+})[2] and bis(imino)pyridylmetal (Fe^{2+} or Co^{2+}) dihalides.[3] To enhance the usefulness of late-transition metal complex pre-catalysts in olefin polymerization, the parallel efforts have been working towards higher activities of the catalytic systems and better properties of the resultant polyolefin materials. Subsequent investigations have approved the production of branched polyethylenes by nickel or palladium systems and linear polyethylenes by iron or cobalt systems.[1] Moreover, iron is by mass the most common element on Earth, therefore extensive studies have focused on the analogous bis(imino)pyridyliron dihalides[4] and catalytic intermediates[5] and mechanisms.[6] Principally the 14e active species is considered for the complex pre-catalysts in olefin polymerization, therefore the iron pre-catalysts favour the tridentate sp^2-nitrogen ligands.[1] In addition to bis(imino)pyridine derivatives (**A**),[3,4] therefore, the alternative and effective model pre-catalysts of iron have been developed through extensively synthesizing tridentate ligands such as 2-imino-1,10-phenanthrolines (**B**),[7] 2-(benzimidazolyl)-1,10-phenanthrolines (**C**),[8] 2-(pyridyl)-1,10-phenanthrolines (**D**),[9] 2-(benzimidazolyl)-6-iminopyridines (**E**),[10] 2-(benzoxazol-2-yl)-6-iminopyridines (**F**),[11] 2-(benzothiazol-2-yl)-6-iminopyridines (**G**),[12] 2-quinoxalinyl-6-iminopyridines (**H**),[13] 2-methyl-2,4-bis(6-iminopyridyl)-*1H*-1,5-benzodiazepines (**I**),[14] 2-(1-arylimino) ethyl)-8-arylimino-5,6,7-trihydroquinolines (**J**),[15] and 1,8-diimino-2,3,4,5,6,7-hexahydroacridines (**K**).[16] Regarding the bis(imino)pyridine derivatives (**A**),[3,4] their iron complex pre-catalysts sometime showed both oligomerization and polymerization of ethylene. The further developed iron complex pre-catalysts bearing double-fused-cyclic 1,8-diimino-2,3,4,5,6,7-hexahydroacridines (**K**) again produced both polyethylene and oligomers;[16] interestingly, their anologs employing mono-fused-cyclic 2-(1-arylimino)ethyl)-8-arylimino-5,6,7-trihydroquinolines (**J**)[15] solely performed ethylene polymerization. Therefore, the ring-stress potentially induces the flexible geometry around the metal core, resulting differences of active species for the multi-component products such as polyethylenes with different molecular weights or oligomers. It is absolutely necessary of the applicable process of complex pre-catalyst to produce either polyethylenes or oligomers instead of the mixture of polyethylene and oligomers. Though complex catalytic system commonly persuades single-site active species in order to have polymers with narrow polydispersity, the variable polydispersity of obtained polyethylenes is highly demanding to fix the industrial requirements. With this in mind, relied on the ring strain and flexibility of cyclic compound, the 2-acetyl-5,6,7,8-tetrahydrocycloheptapyridin-9-one is newly synthesized and used to form new ligand compounds, 2-(1-arylimino)ethyl-9-arylimino-5,6,7,8-tetrahydrocyclohepta-pyridine derivatives, in

this work. The full characterization of both organic compounds and iron complexes have well conducted, the significant influence of seven-numbered ring affects the coordination geometries around the centre iron as well as the catalytic behavior of iron complexes in ethylene polymerization. The molecular structures of representative organic compound and iron complexes are confirmed by the single-crystal X-ray diffraction, meanwhile the DFT calculation is also employed to illustrate the structural flexibility of iron complexes. All iron complexes show high activities towards ethylene polymerization, and their obtained polyethylenes are determined by the GPC and DSC measurements. Herein the detail synthesis and characterizations will be reported as well as the trials of ethylene polymerization of the iron complex pre-catalysts.

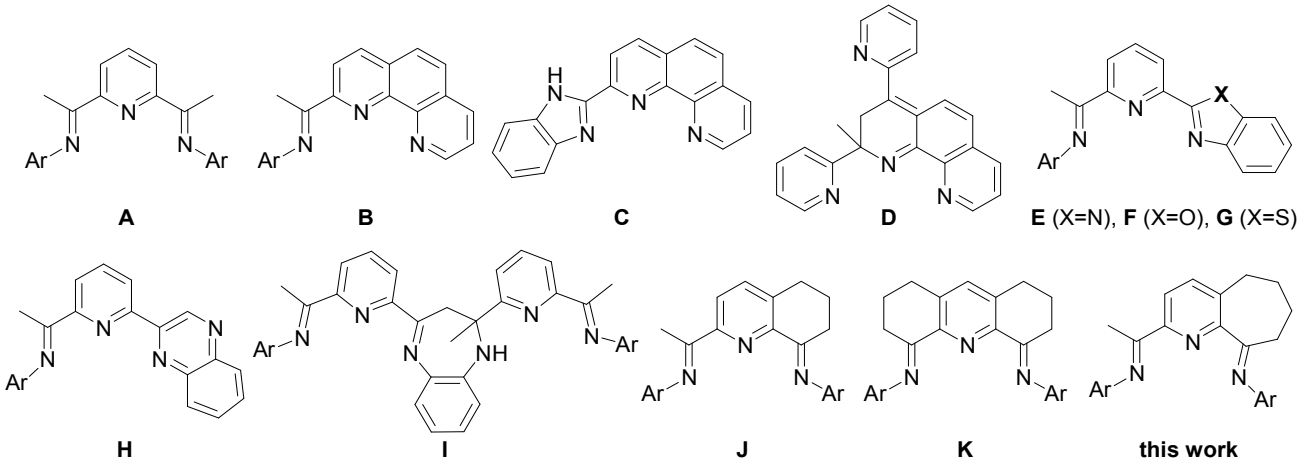

Scheme 1. Ligand frameworks for active iron complex pre-catalysts

Results and Discussion

Synthesis of 2-acetyl-5,6,7,8-tetrahydrocycloheptapyridin-9-one (2).

2-Chloro-5,6,7,8-tetrahydrocycloheptapyridin-9-one, prepared according to the literature,[17] reacts with 1.1 equivalent tributyl(1-ethoxyvinyl)tin for 16 hours in presence of catalytic amount of (dppf)$PdCl_2$ (2.5 mol%) as the Stille coupling reaction (Scheme 2).[18] The resultant solution is hydrolyzed with aqueous HCl, then neutralized with KOH water solution. The organic layer is collected and purified to isolate 2-acetyl-5,6,7,8-tetrahydrocycloheptapyridin-9-one (**2**) in 75%, and the compound **2** is well confirmed by FT-IR, NMR spectroscopy and elemental analysis.

Synthesis and characterization of ligand compounds and their iron complexes.

The condensation reactions of compound **2** with aniline derivatives are conducted in the refluxing *n*-butanol to afford the desired ligand compounds in moderate isolated yield (43–51 %, Scheme 2) according to literature method.[15] The NMR spectra of ligand compounds indicate two isomers for all of them due to double bond migration happened to the imino group linked to the cycloheptane, illustrating major compounds with remaining the imino group (**L**) instead of double bond within cycloheptanic derivatives (**L'**, minor). The isomers with N-H groups are confirmed with the observation around 3360 cm^{-1} in their IR spectra. The single crystals of ligand compound (**L2** and **L2'**) in 2-propanol are obtained and measured by the X-ray diffraction to confirm the structure of *N*-(2-(1-(2,6-diethylphenylimino)ethyl)-5,6,7,8-tetrahydrocycloheptapyridin-9-ylidene)-2,6-diethyl-benzenamine (**L2**) as the sole isomer. The molecular structure of compound **L2** is shown in Figure 1, and its elected bond lengths

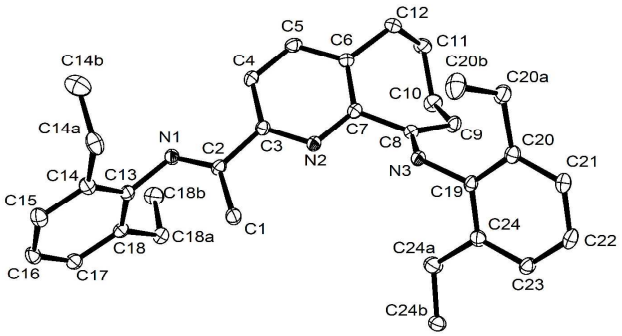

Figure 1. Molecular structure of compound **L2** with thermal ellipsoids at 30% probability. Hydrogen atoms have been omitted for clarity.

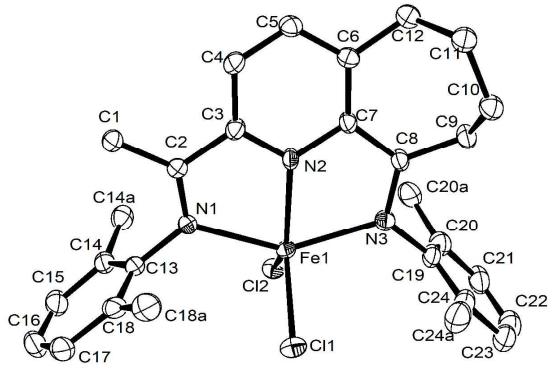

Figure 2. Molecular structure of complex **Fe1** with thermal ellipsoids at 30% probability. Hydrogen atoms have been omitted for clarity.

and angles are tabulated in Table 1. It is necessary to mention that the ^{1}H NMR spectra indicated the ratio of **L2**: **L2'** as 1: 0.31 in its solution, probably the isomer with imono group is likely stable in the solid state. However, DFT calculations on L2 and L2' indicated a marginal energetic difference between two isomers, with the amine-cycloheptene form favored by 1.0 kcal/mol; however, the geometries of the hydrogen migration transition states were not determined.

The stoichiometric reactions of ligand compounds and $FeCl_2$ are individually conducted in ethanol, and the iron complexes, 2,9-bis(imino)-5,6,7,8-tetrahydrocycloheptapyridinolyliron(II) dichlorides (**Fe1**–**Fe5**, Scheme 2), are precipitated and collected. According to their IR spectra, there is no absorption related to the N-H groups, meanwhile the adsorption around 1640 cm^{-1} for $\nu_{C=N}$ in ligand compounds are shifted to around 1610 cm^{-1} within the iron complexes, indicating effective coordination Fe-N_{sp2}. The elemental analysis data confirm the formulae as **L**$FeCl_2$ for all iron complexes. In addition, the molecular structures of complexes **Fe1** and **Fe2** are determined by the single-crystal X-ray diffraction. The molecular structures of complexes **Fe1** and **Fe2** are shown in Figures 2 and 3, and their selected bond lengths and angles are collected in Table 1. Moreover, the DFT calculations are further carried out in order to compare experimental and computational data, and their correspondingly selected bond lengths and angles are listed in Table 1.

As shown in Figure 2, complex **Fe1** possesses a distorted trigonal-bipyramidal geometry at the iron centre, which is similar to its analog, 2-(1-arylimino)ethyl)-8-arylimino-5,6,7-trihydroquinolyl iron dichloride.[15a] The coordination plane is formed with three nitrogens and one iron along with a slight 0.001 Å deviation of the iron, and the coordination plane is nearly perpendicular with a dihedral angle 88.26° to the equatorial plane constituted by the iron atom and two chlorides. Moreover, two phenyl planes bridged through the imino groups are analogously perpendicular to the coordination plane with the dihedral angles of 86.88° and 86.99°, individually. Meanwhile, the lengths of Fe-N bond are slightly different with a shorter Fe-$N_{pyridyl}$ (2.134(4) Å) than the Fe-N_{imino} (2.236(4) and 2.231(4) Å). The shorter bond length, the stronger bonding force, illustrating stronger electronic donation from sp^2-nitrogen to cationic iron; that is also consistent to the different lengths of the two Fe-N_{imino} bonds due to the electronic features of two N_{imino} with the unsymmetrical framework.[12,13,15] Such tendency can also be consistent to the structure calculated by the DFT study.

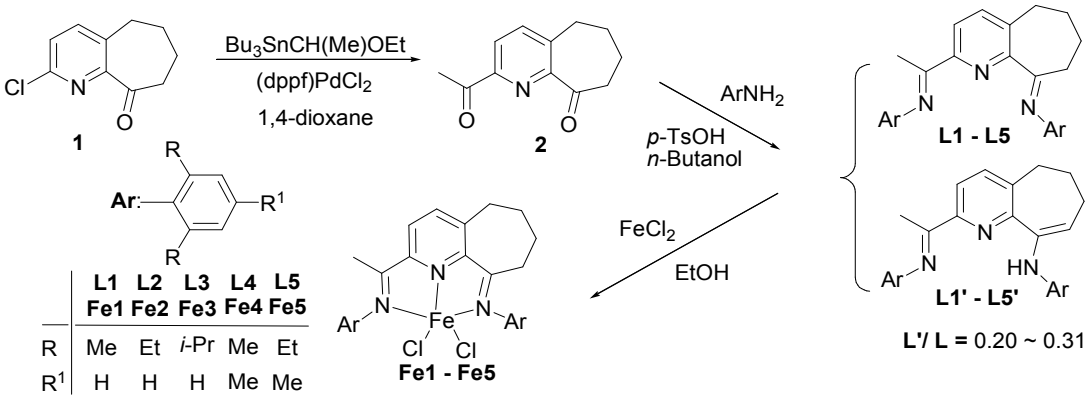

Scheme 2. Synthesis of organic compounds and their iron(II) complexes

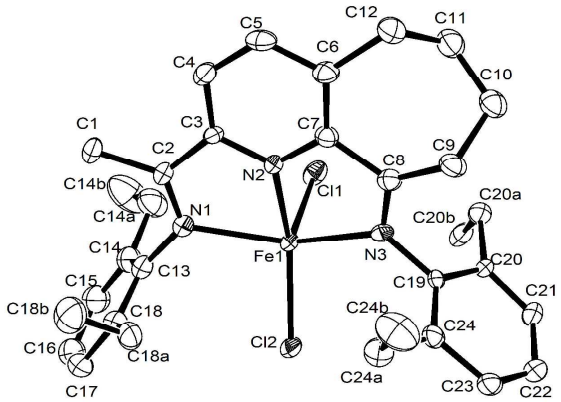

Figure 3. Molecular structure of complex Fe2 with thermal ellipsoids at 30% probability. Hydrogen atoms have been omitted for clarity.

According to the Figure 3, the geometry of complex **Fe2** should be described as approximately distorted square pyramidal around the iron centre, in which three nitrogen atoms and one chloride (Cl2) form the basal plane with the deviation 0.442 Å of the iron from the plane. Interestingly, there are isomeric structures of complex **Fe2** in the solid, causing slight differences of the $FeCl_2$ moiety due to the fused cycloheptane ring, attributing to the flexibility and ring strain of the fused cycloheptane. The energy differences between the three conformers of isolated cycloheptene (considered as a model of a fused cycloheptane ring) do not exceed 3 kcal/mol by DFT calculation. Also, the observed tendency of bond lengths regarding the Fe-$N_{pyridyl}$ and two Fe-N_{imino} are consistent to its above analog **Fe1** as well as literature.[12,13,15]

Ethylene Polymerization

Ethylene Polymerization by Fe1-Fe5/MAO systems.

To activate iron complexes, the most popular co-catalysts reported are methylaluminoxane (MAO) and modified methylaluminoxane (MMAO);[1,15] therefore the optimization of catalytic parameter is explored by the system of **Fe3**/MAO. Because of the exothermic reaction of ethylene polymerization, the reaction temperature is set as 30 ºC for the easy operation, slightly higher than ambient temperature. Various molar ratios of

Al/Fe are investigated (Runs 1–4, Table 2), illustrating the highest activity at the Al/Fe ratio of 2000. Fixing the Al/Fe ratio as 2000, various reaction temperatures are adapted for the ethylene polymerization (Runs 3, 5–8, Table 2), indicating the highest activity observed at 30 ºC. Therefore other complex pre-catalysts are investigated at the Al/Fe ratio of 2000 and temperature 30 ºC (Runs 9–12, Table 2), generally the good activities were achieved.

Table 1. Selected Bond Lengths (Å) and Angles (º) for **L2**, **Fe1** and **Fe2**

	L2		**Fe1**		**Fe2**	
	Experimental	DFT	Experimental	DFT	Experimental	DFT
Bond lengths, Å						
Fe(1)-N(1)			2.236(4)	2.275	2.212(9)	2.265
Fe(1)-N(2)			2.134(4)	2.075	2.107(8)	2.075
Fe(1)-N(3)			2.231(4)	2.198	2.210(8)	2.210
Fe(1)-Cl(1)			2.3035(16)	2.249	2.328(3)	2.276
Fe(1)-Cl(2)			2.3095(15)	2.275	2.260(3)	2.249
N(1)-C(2)	1.282(3)	1.284	1.284(6)	1.300	1.269(15)	1.301
N(3)-C(8)	1.274(3)	1.280	1.352(16)	1.308	1.275(13)	1.308
N(2)-C(3)	1.341(3)	1.339	1.348(6)	1.355	1.345(13)	1.356
N(2)-C(7)	1.343(3)	1.342	1.436(15)	1.364	1.313(13)	1.363
C(2)-C(3)	1.495(4)	1.492	1.485(7)	1.459	1.482(15)	1.459
C(7)-C(8)	1.498(3)	1.500	1.463(14)	1.460	1.512(15)	1.462
Bond angles, °						
N(1)-Fe(1)-N(3)			145.63(15)	141.1	142.5(4)	140.3
N(1)-Fe(1)-N(2)			72.88(14)	72.8	73.2(3)	72.9
N(3)-Fe(1)-N(2)			72.75(15)	73.4	73.2(3)	73.0
N(1)-Fe(1)-Cl(1)			98.49(11)	96.4	99.2(3)	103.0
N(3)-Fe(1)-Cl(1)			101.44(12)	98.1	97.6(2)	101.5
N(2)-Fe(1)-Cl(1)			125.60(12)	141.3	90.6(2)	98.6
N(1)-Fe(1)-Cl(2)			101.51(11)	102.1	100.0(3)	96.0
N(3)-Fe(1)-Cl(2)			99.03(12)	101.6	99.9(2)	99.4
N(2)-Fe(1)-Cl(2)			127.35(12)	99.0	149.0(2)	143.4
Cl(1)-Fe(1)-Cl(2)			107.05(5)	119.7	120.48(14)	118.0
C(8)-N(3)-Fe(1)			118.7(6)	116.5	116.3(7)	116.5
C(19)-N(3)-Fe(1)			123.3(3)	122.8	122.6(6)	122.4
C(2)-N(1)-Fe(1)			117.7(3)	114.9	116.1(8)	115.1
C(13)-N(1)-Fe(1)			123.8(3)	123.8	120.4(7)	124.0
N(1)-C(2)-C(3)	116.5(2)	117.0	115.1(4)	115.3	116.4(10)	115.3
C(2)-C(3)-N(2)	115.1(2)	116.2	114.8(4)	114.8	113.1(9)	114.7
C(3)-N(2)-C(7)	118.0(2)	118.9	118.8(6)	120.4	121.1(9)	120.3
N(2)-C(7)-C(8)	114.7(2)	115.4	113.2(10)	113.0	113.0(9)	113.1
C(7)-C(8)-N(3)	115.9(2)	116.3	114.4(10)	115.2	115.3(9)	114.9

The obtained polyethylenes (PE) were measured by the DSC and GPC measurements. The similar T*m* values were observed, whilst the GPC data indicated PEs with wide polydispersity. To understand the influence of reaction temperature, the GPC traces of PEs, obtained within temperature of 10 ºC to 50 ºC at 1 atm ethylene with the Al/Fe ratio of 2000 (runs 3, 5–8, Table 2), were shown in Figure 4, illustrating the relatively higher molecular weights of PEs as well as a main portion of PEs at lower temperature. Such phenomena indicated more active species formed in addition of fast termination happened at higher temperature.

Considering different pre-catalysts **Fe1**–**Fe5** (runs 3, 9–12, Table 2), the slight influences of substituents were observed. The pre-catalyst **Fe3** (containing R^1=^{i}Pr) showed highest activities and produced PE with higher molecular weight, probably meaning the bulky substituents stabilized the active species. The **Fe2** showed better activity than **Fe1**, however, iron pre-catalysts **Fe4** and **Fe5** bearing additional *para*-methyl substituent resulted lower activity than their analogous pre-catalysts **Fe1** and **Fe2** due to the electronic influences.[19]

Subsequently, the ethylene polymerization was explored with the elevated pressure as 10 atm of ethylene. Again, the parameter optimization was carried out with pre-catalyst **Fe3**, and their results were tabulated in Table 3. Along with ethylene pressure increased, the catalytic activities were significantly improved; moreover, the better thermo-stability was also achieved with optimum temperature as 60 ºC at 10 atm ethylene (Runs 3 and 7, Table 3) instead of 30 ºC at 1 atm ethylene (Run 3, Table 2). Regarding literature iron complexes, the analogous pre-catalysts bearing 1,8-diimino-2,3,4,5,6,7-hexahydroacridine[16] or typical bis(imino)pyridine derivatives[4a] significantly deactivated along

Table 2. Polymerization results by **Fe1**-**Fe5**/MAO at ambient pressure of ethylene [a]

Run	Pre-cat	T /ºC	Al/Fe	PE/g	Act. [b]	T_m /ºC[c]	M_w/Kg. mol^{-1} [d]	M_w/M_n [d]
1	**Fe3**	30	1000	0.52	3.5	128.3	18.0	13.4
2	**Fe3**	30	1500	0.70	4.7	127.9	10.9	10.7
3	**Fe3**	30	2000	1.25	8.3	128.7	68.4	32.5
4	**Fe3**	30	2500	1.11	7.4	127.2	33.5	12.1
5	**Fe3**	10	2000	0.91	6.0	129.4	86.3	34.3
6	**Fe3**	20	2000	0.93	6.2	128.2	75.8	35.2
7	**Fe3**	40	2000	1.17	7.8	127.2	50.0	24.7
8	**Fe3**	50	2000	0.93	6.2	127.9	43.9	24.6
9	**Fe1**	30	2000	1.17	7.8	126.6	24.1	14.8
10	**Fe2**	30	2000	1.22	8.1	126.3	22.9	11.5
11	**Fe4**	30	2000	1.16	7.7	128.5	25.5	14.4
12	**Fe5**	30	2000	0.80	5.3	127.0	24.5	13.6

[a]General conditions: 3 μmol Fe, 30 min, 30 mL toluene, 1 atm ethylene. [b]10^5 gPE·mol^{-1}(Fe)·h^{-1}. [c] Determined by DSC. [d] Determined by GPC.

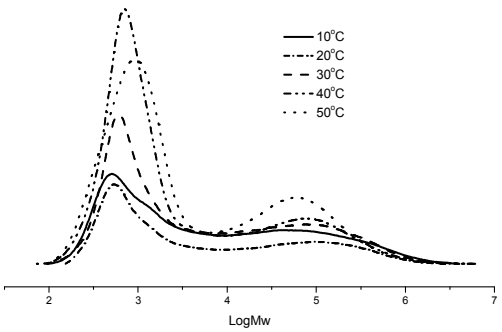

Figure 4. The GPC curves of polyethylene obtained at different temperatures (runs 3, 5–8, Table 2)

with the reaction temperature elevated, though benzhydryl-substituted ligand compounds have been used to enhance the thermo-stability of bis(imino)pyridyliron complexes.[4f-j] The current system showed good thermo-stability at 60 ºC, which is an advantage for industrial application. The optimum temperature is a critical parameter in the olefin polymerization on the basis of highly exothermic process with cooling system of water medium, massive polyolefin process around 80 ºC, but process with temperature lower to 60 ºC operated for the polyethylene with ultrahigh molecular weight. In addition, to maintain high activity, more co-catalyst MAO was also consumed with the ratio up to 2500 regarding iron (Run 7, Table 3).

According to data (Runs 1–5) in Table 3, the optimum temperature was observed as 60 ºC, and all cases showed high activities with slightly decreased activities happened either lower or higher temperature, illustrating that the active species can withstand in the wide temperature toleration. The higher reaction temperature employed, the polyethylenes with lower molecular weights obtained, which were commonly observed.[1] Consistent to its analogous 2-(1-arylimino)ethyl)-8-arylimino-5,6,7-trihydro-quinolyliron pre-catalyst,[15a] the higher reaction temperature used, the narrower polydispersity for the obtained polyethylenes. Probably the active species have been equalized somehow at higher temperature for polyethylenes with narrow molecular weights.

Under 10 atm pressure of ethylene, all pre-catalysts showed similar activities of ethylene polymerization (Runs 7, 9–12, Table 3), with the similar tendency of bulky ligands enhancing the catalytic activities of their correspondent pre-catalysts (Runs 7, 9, and 10, Table 3); however, significant higher activity was observed for pre-catalyst **Fe4**. Their catalytic activities reflected the combined influences of various parameters and nature of ligands used. Moreover, the ^{13}C NMR of several representative polyethylenes also confirmed the high linear feature, which was consistent to the previous observations by iron pre-catalysts.[4f-j,15,20]

Ethylene Polymerization by Fe1–Fe5/MMAO Systems.

Subsequently the co-catalyst MMAO was extensively studied to activate the title iron complexes, and the pre-catalyst **Fe3** was again employed to optimize the reaction parameters. The ethylene polymerization was conducted at ambient pressure of ethylene; the observed results were collected in Table 4. Fixed 2000 Al/Fe ratio, the optimum activity was achieved to 1.15×10^6 g PE·mol^{-1}(Fe)·h^{-1}·atm^{-1} at 20 ºC within the temperature range of 0 ºC to 40 ºC (Runs 1–5, Table 4). Concerning the polyethylenes obtained,

Table 3. Polymerization results by **Fe1**-**Fe5**/MAO at elevated pressure of ethylene [a]

Run	Pre-cat	T /ºC	Al/Fe	PE/g	Act. [b]	T_m /ºC[c]	M_w /Kg·mol^{-1} [d]	M_w/M_n [d]
1	**Fe3**	40	2000	7.00	4.67	129.9	70.0	17.1
2	**Fe3**	50	2000	7.85	5.23	130.1	43.6	9.3
3	**Fe3**	60	2000	13.54	9.03	129.7	30.8	6.7
4	**Fe3**	70	2000	12.81	8.54	130.3	30.7	5.5
5	**Fe3**	80	2000	9.30	6.20	129.0	13.7	3.8
6	**Fe3**	60	1500	8.86	5.91	129.9	38.3	7.7
7	**Fe3**	60	2500	14.28	9.52	129.7	27.5	6.1
8	**Fe3**	60	3000	12.05	8.03	129.7	23.8	5.6
9	**Fe1**	60	2500	10.49	6.99	129.5	14.1	5.6
10	**Fe2**	60	2500	11.10	7.40	129.5	17.9	7.3
11	**Fe4**	60	2500	13.55	9.03	129.5	31.4	9.7
12	**Fe5**	60	2500	10.48	6.99	128.6	15.5	6.3
13	**Fe3**[e]	60	2500	9.90	6.60	130.5	32.6	11.1

[a] General conditions: 3 μmol Fe, 30 min, 100 mL toluene, 10 atm ethylene. [b] 10^6 gPE·mol^{-1}(Fe)·h^{-1}, [c] Determined by DSC. [d] Determined by GPC. [e] 5 atm ethylene.

their molecular weights gradually decrease along with the reaction temperature increased (Figure 5), due to fast chain termination at higher temperature. In comparison with the observations with co-catalyst MAO, the systems with MMAO produced the polyethylene with lower molecular weights, but with narrow polydispersity; more importantly, the system with MMAO performed higher catalytic activity towards ethylene polymerization. It is interpreted the positive influence of MMAO in activating and finely control the active species due to containing bulky *t*-butyl group. The variation on Al/Fe ratio significantly affected the catalytic activity of the current system as well as the property of obtained polyethylenes (Runs 3, 6–8, Table 4); the similar activities were observed with the Al/Fe ratio between 1500 and 2500 (Runs 3, 7 and 8, Table 4), illustrating optimum Al/Fe ratio 2000. It is worthy to emphasize the narrow polydispersity of most polyethylenes obtained, besides the low molecular weights in the range of thousands to tens thousands; the linear polyethylenes (waxes) have been highly demanded as lubricants in finely melting-processes and additives in plastics or paints. Regarding the lifetime of active species (Runs 3, 9–11, Table 4), the correlation between reaction activity and reaction time was in contrary, *i.e.*, the activities decreased along with prolonging the reaction time, indicating there was no inducing time in the catalytic reaction.

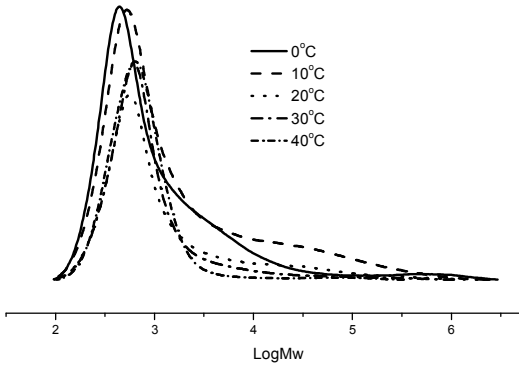

Figure 5. The GPC curves of polyethylene obtained at different temperatures (runs 1–5, Table 4)

Table 4. Polymerization results by **Fe1**-**Fe5**/MMAO at ambient pressure of ethylene [a]

Run	Pre-cat	T /ºC	Al/Fe	PE/g	Act. [b]	T_m/ºC[c]	M_w/Kg·mol^{-1} [d]	M_w/M_n [d]
1	**Fe3**	0	2000	1.62	1.08	122.0	21.7	2.9
2	**Fe3**	10	2000	1.64	1.09	122.2	20.6	6.3
3	**Fe3**	20	2000	1.72	1.15	122.4	13.6	5.3
4	**Fe3**	30	2000	1.42	0.95	120.2	5.9	2.2
5	**Fe3**	40	2000	1.15	0.77	120.9	2.2	1.3
6	**Fe3**	20	1000	0.85	0.57	128.3	73.6	1.6
7	**Fe3**	20	1500	1.62	1.08	125.1	0.9	1.4
8	**Fe3**	20	2500	1.71	1.12	120.1	1.7	1.4
9	**Fe3**[e]	20	2000	1.11	1.48	116.7	0.8	1.5
10	**Fe3**[f]	20	2000	2.17	0.97	124.3	20.6	1.6
11	**Fe1**	20	2000	1.67	1.12	119.9	4.1	1.1
12	**Fe2**	20	2000	1.76	1.17	117.0	3.4	1.3
13	**Fe4**	20	2000	1.36	0.91	118.1	4.0	2.0
14	**Fe5**	20	2000	1.96	1.31	125.1	27.1	1.2

[a] General conditions: 3 μmol Fe, Al/Fe: 2000; 30 mL toluene for 1 atm ethylene, 30 min. [b] 10^6 gPE·mol^{-1}(Fe)·h^{-1}·atm^{-1}. [c] Determined by DSC. [d] Determined by GPC. [e]15min. [f] 45 min.

Under the optimum condition, other iron complexes were investigated for their ethylene polymerization (Runs 11–14, Table 4). In general, the similar activities have been observed for these systems (Runs 3, 11–14, Table 4); however, the slight differences indicated the better activities observed from complexes bearing *ortho*-ethyl substituents on the N_{imino}-phenyl groups, which were consistent to the literature observations.[3a,3b] In parallel, the ethylene polymerization under elevated pressure was also conducted in the assistance of MMAO to achieve very high activities, and their results are tabulated in Table 5. Fixed the Al/Fe ratio 2000 under 10 atm of ethylene, the optimum temperature was observed at 50 ºC with the activity as 15.6 ×10^6 g PE·mol^{-1}(Fe)·h^{-1} (run 3, Table 5); moreover, at higher reaction temperatures (runs 4 and 5, Table 5), the high activities were remained in the range of 10^7 g PE·mol^{-1}(Fe)·h^{-1}, illustrating the catalytic system as both good thermo-stability and high activities. The variation of the Al/Fe ratios (Runs 3, 6–8, Table 5) still confirmed the optimum Al/Fe ratio 2000. Therefore, other iron complexes were also explored under the optimum parameters (Runs 10–13, Table 5). All complex pre-catalysts showed very high activities and fine thermo-stability toward ethylene polymerization (Runs 3, 10–13, Table 5).

Table 5. Polymerization results by **Fe1**–**Fe5**/MMAO at 10 atm ethylene pressure [a]

Run	Pre-cat	T /ºC	Al/Fe	PE/g	Act. [b]	T_m/ºC[c]	M_w/Kg·mol^{-1} [d]	M_w/M_n [d]
1	**Fe3**	30	2000	7.95	5.30	122.3	1.6	1.5
2	**Fe3**	40	2000	8.85	5.90	123.8	3.3	2.0
3	**Fe3**	50	2000	23.40	15.6	130.1	21.9	5.3
4	**Fe3**	60	2000	20.87	13.9	129.9	29.9	6.5
5	**Fe3**	70	2000	17.44	11.6	128.6	19.8	4.9
6	**Fe3**	50	1500	9.42	6.28	125.3	8.4	3.8
7	**Fe3**	50	2500	19.06	12.7	127.6	15.4	5.5
8	**Fe3**	50	3000	18.18	12.2	128.8	19.9	6.2
9	**Fe3**[e]	50	2000	11.26	7.51	125.6	8.5	5.9
10	**Fe1**	50	2000	21.75	14.5	128.1	17.2	7.1
11	**Fe2**	50	2000	21.05	14.0	128.2	11.5	5.9
12	**Fe4**	50	2000	22.76	15.2	128.7	19.1	8.2
13	**Fe5**	50	2000	20.53	13.7	128.9	10.6	5.4

[a] General conditions: 3 μmol Fe, 30 min, 100 mL toluene for 10 atm ethylene. [b]10^6 gPE·mol^{-1}(Fe)·h^{-1}. [c] Determined by DSC. [d] Determined by GPC. [e] 5 atm ethylene.

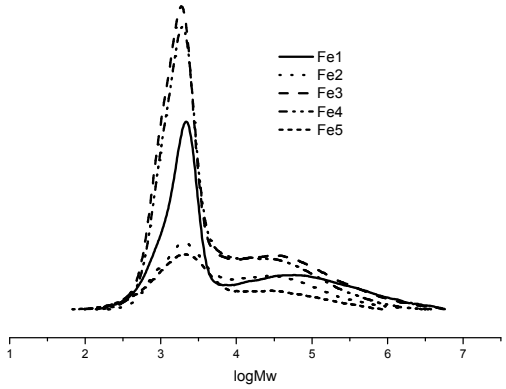

Figure 6. The GPC curves of the obtained polyethylenes varied by the iron pre-catalysts (runs 3, 10–13, Table 5).

Regarding the properties of obtained polyethylenes (Runs 3, 10–13, Table 5), the GPC measurements showed molecular weights about tens thousands with bimodal features (Figure 6). Though there were no direct evidences yet, it was assumed the different active species created due to the fused-cycloheptance, which affected location of one-imino group linked. The feature of most homogeneous pre-catalysts is favour to single-site species; the new challenges are to create dual or multi-site species with being finely controlled from the nature of ligands used. The tunable catalytic species with multi-active sites have been highly demanding for their industrial applications. Therefore the current systems, besides the high activities and good thermo-stability, are under further investigations through optimizing their reaction parameters and carefully characterizing the obtained polyethylenes for their applications.

Conclusion

A series of 2,9-bis(arylimino)-5,6,7,8-tetrahydrocyclohepta-pyridine iron(II) complexes have been synthesized and fully characterized. Molecular structures of compounds **L2**, **Fe1** and **Fe2** were measured by the single-crystal X-ray diffraction and DFT study, observing their geometries of complex **Fe1** as a distorted trigonal bipyramidal and complex **Fe2** as a distorted square pyramidal. On the basis of ring strain of fused cycloheptapyridine ligand, several isomers were clearly observed in the solid state of complex **Fe2**; however, the DFT study indicated that the energies of three cycloheptene conformers fall within 3 kcal/mol. Upon treatment with either MAO or MMAO, all pre-catalysts **Fe1**–**Fe5** exhibited very high activities toward ethylene polymerization without any trace of oligomers, up to 1.56×10^6 g PE·mol^{-1}(Fe)·h^{-1}·atm^{-1} at 50 ºC under 10 atm ethylene. Principally the catalytic systems with MMAO performed higher activities than their analogs with MAO; moreover, the systems with MMAO produced polyethylenes with lower molecular weights and narrower polydispersity. Finely controlling reaction parameters, the obtained polyethylenes would be modified for the molecular weights and polydispersity. This is a rare case of one complex model to achieve single-site to multi-site species in ethylene polymerization. Further investigations are worthily conducted to enhance their catalytic activities and produce useful polyethylenes, and then the practice of complex pre-catalysts would be provided for the industrial

consideration.

Experimental

General Considerations.

All manipulations of air- and/or moisture-sensitive operations were processed in a nitrogen atmosphere using standard Schlenk techniques. Toluene was refluxed over sodium and distilled under nitrogen prior to use. Methylaluminoxane (1.46 M solution in toluene) and modified methylaluminoxane (MMAO, 1.93 M in *n*-heptane) were purchased from Akzo Nobel Corp. High-purity ethylene was purchased from Beijing Yanshan Petrochemical Co. and used as received. Other reagents were purchased from Aldrich, Acros, or local suppliers. NMR spectra were recorded on Bruker DMX 400 MHz instrument at ambient temperature using TMS as an internal standard. IR spectra were recorded on a Perkin-Elmer System 2000 FT-IR spectrometer. Elemental analysis was carried out using a Flash EA 1112 microanalyzer. Molecular weights and molecular weight distribution (MWD) of polyethylenes were determined by a PL-GPC220 at 150 ºC, with 1,2,4-trichlorobenzene as the solvent. DSC trace and melting points of polyethylene were obtained from the second scanning run on DSC Q2000 at a heating rate of 10 ºC/min to 160 ºC.

Synthesis of 2-acetyl-5,6,7,8-tetrahydrocyclohepta[b]pyridin-9-one (2).

2-chloro-5,6,7,8-tetrahydrocyclohepta[b]pyridin-9-one **1** (170 mmol, 33.3 g), tributyl(1-ethoxyvinyl)tin (187 mmol, 67.7 g), $Pd(dppf)Cl_2$ (2.5 mol%, 3.73 g), and 330 ml of 1,4-dioxane was added to a 1000 ml three-necked jacketed flask. The mixture was refluxed for 16 h under N_2, after cooling to room temperature, added 300 ml of 1.2M HCl aqueous slowly, and determined by GC. After hydrolysis was finished, added KOH aqueous to make the aqueous neutral, the organic layer was separated and removed under reduced pressure, then added 400ml ethyl acetate and washed with KF solution (0.3 M, 100 ml × 3). Finally, the organic layer was separated again and dried over anhydrous Na_2SO_4, concentrated in vacuo to afford the crude product. The residue was purified by silica gel chromatography to afford **2** 25.9 g (yield 75.0%) as a light yellow solid. Mp: 88-90 ºC. ^{1}H NMR (400 MHz, $CDCl_3$): δ 7.72 (d, *J* = 3.2 Hz, 1H, Py-H), 7.70 (d, *J* = 3.2 Hz, 1H, Py-H), 4.30 (t, *J* = 6.6 Hz, 2H, -CH_2-), 1.73-1.68 (m, 2H, -CH_2-), 1.46-1.41 (m, 2H, -CH_2-), 1.25 (s, 3H, CH_3), 0.95 (t, *J* = 6.6 Hz, 2H, -CH_2-). ^{13}C NMR (100 MHz; $CDCl_3$; TMS): δ 204.7, 199.6, 154.8, 152.2, 139.4, 138.7, 123.2, 40.5, 31.1, 25.6, 24.9, 21.6.

Synthesis of (E)-N-(2-((E)-1-(2,6-dimethylphenylimino)ethyl)-5,6,7,8-tetra-hydrocyclohepta[b]pyridin-9-ylidene)-2,6-dimethylbenzenamine (L1) and (E)-N- (2,6-dimethylphenyl)-2-((E)-1-(2,6-dimethylphenylimino)ethyl)-6,7-dihydro-*5H*-cyclohepta[b]pyridin-9-amine (L1').

2,6-Dimethylaniline (0.30 g, 2.5 mmol) was added to a solution of 2-acetyl-5,6,7,8-tetrahydrocycloheptapyridin-9-one (2) (0.20 g, 1.0 mmol) with a catalyst p-toluenesulfonic acid (20.0 mg, 0.1 mmol) in 40 mL of *n*-butanol. The mixture was stirred at reflux temperature for 6 h. The solvent was evaporated under reduced pressure, and the residue was then purified by silica gel chromatography to afford 0.21 g (yield 51.3%) a yellow oil with crude molar ratio of L1: L1' = 1: 0.23 (detected by ^{1}H NMR). ^{1}H NMR (400 MHz, CD_2Cl_2): δ 8.36 (d, *J* = 8.0 Hz, 1H, L1-Py-H), 8.25 (d, *J* = 8.0 Hz, 1H, L1'-Py-H), 7.64 (d, *J* = 8.0 Hz, 1H, L1-Py-H), 7.52 (d, *J* = 8.0 Hz, 1H, L1'-Py-H), 7.04 (m, 4H, L1-Ar-H), 6.98 (d, *J* = 7.8 Hz, 4H, L1'-Ar-H), 6.90 (t, *J* = 7.6 Hz, 2H, L1-Ar-H), 6.85 (t, *J* = 7.8 Hz, 2H, L1'-Ar-H), 6.41 (s, 1H, L1'-NH-), 4.59 (t, *J* = 6.8 Hz, 1H, L1'-CH=), 2.92 (t, *J* = 6.0 Hz, 2H, L1-CH_2-), 2.76 (t, *J* = 6.4 Hz, 2H, L1'-CH_2-), 2.34 (s, 3H, L1'-CH_3), 2.28 (t, *J* = 5.6 Hz, 2H, L1-CH_2-), 2.20 (s, 3H, L1-CH_3), 2.14 (s, 6H, 2 x L1-Ph-CH_3), 2.00 (s, 6H, 2 x L1-Ph-CH_3), 2.09-2.04 (m, 2H, L1-CH_2-), 1.94-1.88 (m, 2H, L1-CH_2-). ^{13}C NMR (100 MHz; CD_2Cl_2; TMS): δ 173.0, 167.3, 156.5, 154.6, 149.2, 148.5, 138.3, 137.5, 136.3, 128.4, 127.9, 127.8, 127.1, 125.9, 125.5, 125.1, 122.9, 121.9, 121.3, 120.6, 38.9, 33.5, 32.0, 27.4, 26.6, 26.2, 24.3, 18.4, 18.1, 17.8, 17.7, 16.2. FT-IR (KBr, cm^{-1}): 3374(ν_{N-H}), 2928 (m), 2856(w), 1643(s), 1593(m), 1564(w), 1464(s), 1440(s), 1362(m), 1312(w), 1253(w), 1200(s), 1163(m), 1124(m), 1090(m), 1032(w), 847(w), 808(w), 762(vs), 691(w). Anal. Calcd. For $C_{28}H_{31}N_3$: C, 82.01; H, 7.63; N, 10.26. Found: C, 81.61; H, 7.75; N, 10.48.

Synthesis of (E)-N-(2-((E)-1-(2,6-diethylphenylimino)ethyl)-5,6,7,8-tetrahydrocyclohepta[b]pyridin-9-ylidene)-2,6-diethylbenzenamine (L2) and (E)-N-(2,6-diethylphenyl)-2-((E)-1-(2,6-diethylphenylimino)ethyl)-6,7-dihydro-*5H*-cyclohepta[b]pyridin-9- amine (L2').

Using the same procedure as for the synthesis of L1/L1', L2/L2' was obtained as a yellow powder (0.20 g, 42.9%) with crude molar ratio of L2: L2' = 1: 0.31 (detected by ^{1}H NMR). Mp: 130-131 ºC. ^{1}H NMR (400 MHz, CD_2Cl_2): δ 8.36 (d, *J* = 8.0 Hz, 1H, L2-Py-H), 8.25 (d, *J* = 8.0 Hz, 1H, L2'-Py-H), 7.69 (d, *J* = 8.0 Hz, 1H, L2'-Py-H), 7.64 (d, *J* = 8.0 Hz, 1H, L2-Py-H), 7.12 (m, 4H, Ar-H), 7.00 (t, *J* = 7.6 Hz, 2H, Ar-H), 6.41 (s, 1H, L2'-NH-), 4.61 (t, *J* = 6.8 Hz, 1H, L2'-CH=), 2.95 (t, *J* = 5.2 Hz, 2H, L2-CH_2-), 2.76 (t, *J* = 7.6 Hz, 2H, L2'-CH_2-), 2.56 (m, 2H, L2-Ar-CH_2-), 2.49-2.29 (m, 8H, 4 x L2-Ar-CH_2-), 2.22 (s, 3H, L2-CH_3), 2.06 (m, 2H, L2'-CH_2-), 1.93 (m, 2H, L2'-CH_2-), 1.84 (m, 2H, L2-CH_2-), 1.65 (m, 2H, L2-CH_2-), 1.21 (t, *J* = 7.6 Hz, 6H, 2 x L2-CH_3), 1.11 (t, *J* = 7.6 Hz, 6H, 2 x L2-CH_3), 1.08 (t, *J* = 7.6 Hz, 6H, 2 x L2'-CH_3), 1.01 (t, *J* = 7.6 Hz, 6H, 2 x L2'-CH_3). ^{13}C NMR (100 MHz; CD_2Cl_2; TMS): δ 172.6, 167.1, 156.5, 154.6, 148.2, 147.6, 141.7, 137.4, 136.2, 131.4, 130.9, 126.7, 126.2, 126.1, 126.0, 124.6, 123.2, 121.3, 32.1, 31.8, 26.1, 24.8, 24.7, 24.6, 24.0, 16.6, 15.2, 13.8, 13.7, 12.8. FT-IR (KBr, cm^{-1}): 3372(ν_{N-H}), 2962(m), 2930(m), 2867(w), 1644(s), 1585(w), 1565(w), 1453(s), 1362(m), 1318(w), 1250(w), 1195(m), 1164(m), 1125(m), 1098(m), 961(w), 871(m), 801(w), 763(vs), 692(w). Anal. Calcd. For $C_{32}H_{40}N_3$: C, 82.53; H, 8.44; N, 9.02. Found: C, 82.16; H, 8.45; N, 8.78.

Synthesis of (E)-N-(2-((E)-1-(2,6-diisopropylphenylimino)-ethyl)-5,6,7,8-tetrahydrocyclohepta[b]pyridin-9-ylidene)-2,6-diisopropylbenzenamine (L3) and (E)-N-(2,6-diisopropylphenyl)-2-((E)-1-(2,6-diisopropylphenylimino)-ethyl)-6,7-di-hydro-5H-cyclohepta[b]pyridin-9-amine (L3').

Using the same procedure as for the synthesis of L1/L1', L3/L3' was obtained as a yellow powder (0.24 g, 46.0%) with crude molar ratio of L3: L3' = 1: 0.20 (detected by ^{1}H NMR). Mp: 184-186 ºC. ^{1}H NMR (400 MHz, CD_2Cl_2): δ 8.36 (d, *J* = 8.0 Hz, 1H, L3-Py-H), 8.23 (d, *J* = 7.6 Hz, 1H, L3'-Py-H), 7.69 (d, *J* = 7.6

Hz, 1H, L3'-Py-H), 7.65 (d, J = 8.0 Hz, 1H, L3-Py-H), 7.14 (m, 4H, L3-Ar-H), 7.05 (t, J = 7.6 Hz, 2H, L3-Ar-H), 6.32 (s, 1H, L3'-NH-), 4.60 (t, J = 6.8 Hz, 1H, L3'-CH=), 3.41 (m, 2H, L3'-CH-), 2.99 (m, 2H, L3-CH-), 2.92 (t, J = 6.0 Hz, 2H, L3-CH_2-), 2.85 (m, 2H, L3'-CH-), 2.75 (m, 2H, L3-CH-), 2.50 (t, J = 6.4 Hz, 2H, L3'-CH_2-), 2.31 (t, J = 6.0 Hz, 2H, L3-CH_2-), 2.22 (s, 3H, L3-CH_3), 2.04 (m, 2H, L3'-CH_2-), 1.96 (m, 2H, L3'-CH_2-), 1.83 (m, 2H, L3-CH_2-), 1.65 (m, 2H, L3-CH_2-), 1.25 (d, J = 6.8 Hz, 24H, 8 x L3'-Ph-CH_3), 1.15-1.10 (m, 24H, 8 x L3-Ph-CH_3). ^{13}C NMR (100 MHz; CD_2Cl_2; TMS): δ 172.9 167.1, 156.4, 154.7, 146.1, 137.3, 136.1, 135.9, 135.6, 123.6, 123.5, 123.2, 123.0, 121.3, 32.2, 31.7, 28.3, 28.2, 26.1, 23.7, 23.1, 22.7, 22.5, 16.9. FT-IR (KBr, cm^{-1}): 3374(ν_{N-H}), 2958(m), 2865(w), 1643(s), 1585(w), 1459(vs), 1385(w), 1360(m), 1324(w), 1237(w), 1189(m), 1120(m), 1054(w), 961(w), 863(m), 796(w), 762(vs), 693(w). Anal. Calcd. For $C_{36}H_{47}N_3$: C, 82.87; H, 9.08; N, 8.05. Found: C, 82.39; H, 9.08; N, 7.78.

Synthesis of (E)-N-(2-((E)-1-(mesitylimino)ethyl)-5,6,7,8-tetrahydro-cyclohepta[b]pyridin-9-ylidene)-2,4,6-trimethyl-benzenamine (L4) and (E)-N-mesityl-2-((E)-1-(mesitylimino)ethyl)-6,7-dihydro-5H-cyclohepta[b]pyridin-9-amine (L4').

Using the same procedure as for the synthesis of L1/L1', L4/L4' was obtained as a yellow oil (0.22 g, 50.3%) with crude molar ratio of L4: L4' = 1: 0.21 (detected by ^{1}H NMR). ^{1}H NMR (400 MHz, CD_2Cl_2): δ 8.32 (d, J = 8.0 Hz, 1H, L4-Py-H), 8.21 (d, J = 8.0 Hz, 1H, L4'-Py-H), 7.66 (d, J = 8.0 Hz, 1H, L4'-Py-H), 7.61 (d, J = 8.0 Hz, 1H, L4-Py-H), 6.90 (s, 4H, L4'-Ar-H), 6.86 (s, 2H, L4-Ar-H), 6.85 (s, 2H, L4-Ar-H), 6.29 (s, 1H, L4'-NH-), 4.55 (t, J = 6.8 Hz, 1H, L4'-CH=), 2.89 (t, J = 6.4 Hz, 2H, L4-CH_2-), 2.73 (t, J = 6.4 Hz, 2H, L4'-CH_2-), 2.28 (t, J = 4.8 Hz, 2H, L4-CH_2-), 2.25 (s, 6H, 2 x L4-Ph-CH_3), 2.22 (s, 6H, 2 x L4'-Ph-CH_3), 2.16 (s, 3H, L4-CH_3), 2.14 (s, 3H, L4'-CH_3), 2.08 (s, 6H, 2 x L4-Ph-CH_3), 2.06 (s, 6H, 2 x L4'-Ph-CH_3), 1.96 (s, 6H, 2 x L4'-Ph-CH_3), 1.95 (s, 6H, 2 x L4-Ph-CH_3), 1.90 (m, 2H, L4-CH_2-), 1.62 (m, 2H, L4-CH_2-). ^{13}C NMR (100 MHz; CD_2Cl_2; TMS): δ 173.4, 167.5, 156.6, 154.7, 146.7, 146.6, 146.0, 138.2, 137.4, 136.1, 132.1, 130.9, 129.0, 128.8, 128.6, 128.5, 127.8, 125.4, 124.9, 121.2, 120.4, 39.0, 35.6, 32.9, 32.0, 31.9, 27.6, 26.6, 24.4, 20.8, 20.6, 20.4, 18.4, 18.0, 17.7, 16.4, 16.1. FT-IR (KBr, cm^{-1}): 3368(ν_{N-H}), 2932(s), 2857(m), 1644(s), 1565(w), 1479(s), 1444(s), 1365(m), 1309(w), 1260(w), 1212(s), 1146(m), 1123(m), 1082(w), 1033(w), 853(w), 794(w), 736(w). Anal. Calcd. For $C_{30}H_{35}N_3$: C, 82.34; H, 8.06; N, 9.60. Found: C, 81.94; H, 8.11; N, 9.29.

Synthesis of (E)-N-(2-((E)-1-(2,6-diethyl-4-methylphenyl-imino)ethyl)-5,6,7,8-tetrahydrocyclohepta[b]pyridin-9-ylidene)-2,6-diethyl-4-methylbenzenamine (L5) and (E)-N-(2,6-diethyl-4-methylphenyl)-2-((E)-1-(2,6-diethyl-4-methyl-phenylimino)ethyl)-6,7-dihydro-5H-cyclohepta[b]pyridin-9-amine (L5').

Using the same procedure as for the synthesis of L1/L1', L5/L5' was obtained as a yellow oil (0.24 g, 48.6%) with crude molar ratio of L5: L5' = 1: 0.29 (detected by ^{1}H NMR). ^{1}H NMR (400 MHz, CD_2Cl_2): δ 8.32 (d, J = 8.0 Hz, 1H, L5-Py-H), 8.21 (d, J = 8.0 Hz, 1H, L5'-Py-H), 7.67 (d, J = 8.0 Hz, 1H, L5'-Py-H), 7.62 (d, J = 7.6 Hz, 1H, L5-Py-H), 6.95 (s, 4H, L5'-Ar-H), 6.91 (s, 2H, L5-Ar-H), 6.90 (s, 2H, L5-Ar-H), 6.89 (s, 2H, L5'-Ar-H), 6.28 (s, 1H, L5'-NH-), 4.56 (t, J = 6.8 Hz, 1H, L5'-CH=), 2.91 (t, J = 6.0 Hz, 2H, L5-CH_2-), 2.74 (t, J = 6.4 Hz, 2H, L5'-CH_2-), 2.58 (m, 2H, L5-Ar-CH_2-), 2.43-2.32 (m, 8H, 4 x L5-Ar-CH_2-), 2.29 (s, 6H, 2 x L5-Ph-CH_3), 2.19 (s, 3H, L5-CH_3), 2.13 (s, 3H, L5'-CH_3), 2.03 (m, 2H, L5'-CH_2-), 1.92 (m, 2H, L5'-CH_2-), 1.83 (m, 2H, L5-CH_2-), 1.64 (m, 2H, L5-CH_2-), 1.18 (t, J = 7.6 Hz, 6H, 2 x L5-CH_3), 1.08 (t, J = 7.6 Hz, 6H, 2 x L5-CH_3), 0.98 (t, J = 7.6 Hz, 6H, 2 x L5'-CH_3), 0.86 (t, J = 7.6 Hz, 6H, 2 x L5'-CH_3). ^{13}C NMR (100 MHz; CD_2Cl_2; TMS): δ 172.9, 167.2, 162.1, 156.4, 154.7, 149.1, 144.8, 137.2, 135.9, 132.2, 132.1, 131.1, 130.7, 127.3, 126.8, 126.6, 125.2, 121.0, 45.7, 31.8, 31.7, 29.6, 26.0, 24.6, 24.5, 24.4, 23.8, 20.6, 16.4, 15.2, 13.7, 13.6, 12.8. FT-IR (KBr, cm^{-1}): 3372(ν_{N-H}), 2963(m), 2929(m), 2865(w), 1641(s), 1564(w), 1458(vs), 1364(m), 1314(w), 1259(w), 1206(m), 1145(m), 1123(m), 1079(m), 964(w), 883(w), 856(s), 805(w), 737(m), 699(w). Anal. Calcd. For $C_{34}H_{43}N_3$: C, 82.71; H, 8.78; N, 8.51. Found: C, 82.49; H, 8.74; N, 8.09.

Synthesis of (E)-N-(2-((E)-1-(2,6-dimethylphenylimino)ethyl)-5,6,7,8-tetra-hydrocyclohepta[b]pyridin-9-ylidene)-2,6-dimethylbenzenamine iron(II) dichloride (Fe1).

The ligand **L1/L1'** (0.12 g, 0.23 mmol) and the metal salt $FeCl_2{\cdot}4H_2O$ (0.04 g, 0.20 mmol) were added together in a Schlenk tube, 6 ml of degassed of freshly distilled ethanol was injected into this tube, the mixture was rapidly stirred at room temperature for 12 h, then Et_2O was added to the reaction to precipitate the complex **Fe1**, after filtering, the precipitate was washed with Et_2O (3 × 5 mL) and dried under vacuum to give the product as dark blue powder (0.09 g, 83.3%). FT-IR (KBr, cm^{-1}): 2917(m), 2863(w), 1620(m), 1583(m), 1473(s), 1374(m), 1259(m), 1231(w), 1202(m), 1092(w), 853(w), 773(s). Anal. Calcd. for $C_{28}H_{31}Cl_2FeN_3$: C, 62.71, H, 5.83, N, 7.83; Found: C, 62.34, H, 5,71, N, 7.45.

Synthesis of (E)-N-(2-((E)-1-(2,6-diethylphenylimino)ethyl)-5,6,7,8-tetrahydrocyclohepta[b]pyridin-9-ylidene)-2,6-diethylbenzenamine iron(II) dichloride (Fe2).

By the above procedure, **Fe2** was isolated as blue powder in 81.4% yield. FT-IR (KBr, cm^{-1}): 2966(m), 2933.0(m), 2869(w), 1606(w), 1594(w), 1566(w), 1448(s), 1373(m), 1316(w), 1264(m), 1193(m), 1141(w), 1111(w), 1056(w), 850(m), 806(m), 775(s), 707(w). Anal. Calcd. for $C_{32}H_{40}Cl_2FeN_3$: C, 64.88, H,6.64, N, 7.09; Found: C, 64.52, H, 6.60, N, 6.95.

Synthesis of (E)-N-(2-((E)-1-(2,6-diisopropylphenylimino)-ethyl)-5,6,7,8-tetrahydrocyclohepta[b]pyridin-9-ylidene)-2,6-diisopropylbenzenamine iron(II) dichloride (Fe3).

By the above procedure, **Fe3** was isolated as blue powder in 84.4% yield. FT-IR (KBr, cm^{-1}): 2963(s), 2865(m), 1607(w), 1566(m), 1461(s), 1367(m), 1316(m), 1254(m), 1188(s), 1110(m), 1051(w), 937(w), 847(m), 800(m), 771(s), 710(w). Anal. Calcd. for $C_{36}H_{47}Cl_2FeN_3$: C, 66.67, H, 7.30, N, 6.48; Found: C, 66.26, H, 7.34, N, 6.42.

Synthesis of (E)-N-(2-((E)-1-(mesitylimino)ethyl)-5,6,7,8-tetrahydrocyclohepta[b]pyridin-9-ylidene)-2,4,6-trimethyl-benzenamine iron(II) dichloride (Fe4).

By the above procedure, **Fe4** was isolated as light green powder in 42.6% yield. FT-IR (KBr, cm^{-1}): 2920(m), 2863(w), 1612(w), 1572(m), 1477(m), 1452(m), 1374(m), 1309(w), 1259(m),

1211(s), 1156(w), 1117(w), 1085(w), 1036(m), 855(s), 815(w), 742(w). Anal. Calcd. for $C_{30}H_{35}Cl_2FeN_3$: C, 63.84, H, 6.25, N, 7.45; Found: C, 63.77, H, 6.12, N, 7.40.

Synthesis of (E)-N-(2-((E)-1-(2,6-diethyl-4-methylphenylimino)ethyl)-5,6,7,8-tetrahydrocyclohepta[b]pyridin-9-ylidene)-2,6-diethyl-4-methylbenzenamine iron(II)dichloride (Fe5).

By the above procedure, **Fe5** was isolated as dark blue powder in 54.0% yield. FT-IR (KBr, cm^{-1}): 2964(m), 2933(m), 2866(w), 1611(w), 1579(w), 1561(w), 1456(s), 1368(m), 1340(w), 1257(m), 1206(m), 1183(m), 1160(w), 1120(w), 879(w), 856(s), 792(w). Anal. Calcd. for $C_{34}H_43Cl_2FeN_3$: C, 65.81, H, 6.99, N, 6.77; Found: C, 65.55, H, 6.78, N, 6.29.

Procedure for Ethylene Polymerization.

Ethylene polymerization was carried out in a stainless steel autoclave (250 mL capacity) equipped with an ethylene pressure control system, a mechanical stirrer and a temperature controller. The autoclave was vacuumized and replaced by ethylene, then repeated the operation for three times. And when the desired reaction temperature was reached, under ethylene atmosphere, toluene, co-catalyst, and a toluene solution of the catalytic precursor (the total volume was 100 mL) were injected into the autoclave by using syringes, and then the ethylene pressure was increased to 10 atm, and maintained at this level with constant feeding of ethylene. After the desired reaction period, the reactor was cooled with ice-water bath and the excess ethylene was vented. The resultant mixture was poured into 10% HCl/ethanol solution, and the polymer was collected and washed with ethanol several times and dried under vacuum to constant weight.

X-ray Crystallographic Studies.

Single crystals of the iron(II) complexes **L2**, **Fe1** and **Fe2** suitable for X-ray diffraction analysis were obtained by slow diffusion of diethyl ether into their dichloromethane solutions under nitrogen atmosphere at room temperature, respectively. Data collection for **L2** was carried out on Rigaku MM007-HF Saturn 724 + CCD diffractometer with confocal mirror monochromated Mo Kα radiation (λ = 0.71073 Å), whilst those for **Fe1** and **Fe2** were carried out on Rigaku Saturn 724 + CCD diffractometer with graphite- monochromated Mo Kα radiation (λ = 0.71073 Å). Cell parameters were obtained by global refinement of the positions of all collected reflections. Intensities were corrected for Lorentz and polarization effects and empirical absorption. The structures were solved by direct methods and refined by full-matrix least squares on F^2. All hydrogen atoms were placed in calculated positions. Structure solution and refinement were performed by using the SHELXL-97 package.[21] Within the structure refinement of **Fe1**, the SQUEEZE option of the program PLATON[22] was used to remove free solvent molecules of dichloromethane, which made no influence on the structure of **Fe1**. Details of the X-ray structure determinations and refinements for **L2**, **Fe1** and **Fe2** are provided in Table 6.

Computational Details

All the calculations utilized the BP86 functional[23,24] with the Vosko, Wilk, and Nusair parametrization of the electron gas[25]. A valence triple-ζ Slater-type orbital (STO) basis set with polarization function was applied to the Fe atom, while for the H, C, N, and Cl atoms a double-ζ basis set augmented with polarization function were used. The frozen core approximation applied extended up to 3p for Fe, 2p for Cl and 1s for C and N. On the grounds of the experimental findings[3], the spin state of the iron (II) complexes was quintet. The convergence criteria for geometry optimizations were 0.0001 au in the energy and 0.001 au·Å^{-1} or au·rad^{-1} in the gradient. The integration parameter used was 5.0. Analytical frequencies were calculated only for free ligands. DFT calculations were carried out using the ADF 2013 program.[26-28]

Table 6. Crystal data and Structure Refinement for **L2, Fe1** and **Fe2**.

	L2	Fe1	Fe2
Cryst color	yellow	blue	blue
Empirical formula	$C_{32}H_{40}N_3$	$C_{28}H_{31}Cl_2FeN_3$	$C_{32}H_{39}Cl_2FeN_3$
Formula weight	466.67	536.31	592.41
T (K)	173	173 (2)	173 (2)
wavelength (Å)	0.71073	0.71073	0.71073
cryst syst	monoclinic	triclinic	monoclinic
space group	P21/c	P-1	Cc
a (Å)	7.800 (16)	10.195(2)	38.289 (8)
b (Å)	14.869(3)	13.079(3)	34.676(7)
c (Å)	23.458(5)	22.311(5)	18.386(4)
α (°)	90.00	94.64(3)	90 (0)
β (°)	92.03(3)	92.62(3)	99.36 (3)
γ (°)	90.00	102.15(3)	90 (0)
V (Å3)	2718.9(10)	2892.6(10)	24087(8)
Z	4	4	32
Dcalcd. (mgm-3)	1.140	1.232	1.307
μ (mm-1)	0.066	0.725	0.704
F(000)	1012.0	1120.0	9984.0
cryst size (mm)	0.50×0.25×0.12	0.34×0.25×0.11	0.61×0.39×0.39
θ range (°)	3.48 - 51.36	0.92 - 25.00	0.8 - 25.00
limiting indices	-8 ≤ h ≤ 9 -18 ≤ k ≤ 16 -26 ≤ l ≤ 28	-11 ≤ h ≤ 12 -15 ≤ k ≤ 15 -26 ≤ l ≤ 24	-45 ≤ h ≤ 45 -41≤ k ≤ 41 -21 ≤ l ≤ 21
no. of rflns collected	17021	22346	71381
no. unique rflns [R(int)]	5165(0.0702)	10110(0.0632)	40384(0.0624)
Completeness to θ (%)	99.8 (θ = 25.68)	99.1 (θ = 25.00)	99.8 (θ = 25.00)
Goodness of fit on F2	1.002	1.067	1.092
Final R indices [I > 2σ(I)]	R1 = 0.0781 wR2 = 0.1568	R1 = 0.0731 wR2 = 0.1910	R1 = 0.0977 wR2 = 0.2150
R indices (all data)	R1 = 0.0934 wR2 = 0.1679	R1 = 0.0900 wR2 = 0.2035	R1 = 0.1249 wR2 = 0.2499
largest diff peak and hole (e Å-3)	0.41 and -0.58	0.54 and -0.49	0.86 and -0.54

Acknowledgements

This work is supported by NSFC Nos. 21473160, 21374123, 21204092 and U1362204. ZF thanks the Chinese Academy of Sciences for the Visiting Scientist Fellowship. The computational study was supported in part by the PL-Grid Infrastructure at the Wroclaw Supercomputing and Networking Centre as well as Academic Computer Centre CYFRONET AGH.

Notes and references

[a] *College of Chemical Engineering, Zhejiang University of Technology, Hangzhou 310014, China;*
[b] *Key laboratory of Engineering Plastics and Beijing National Laboratory for Molecular Science, Institute of Chemistry, Chinese Academy of Sciences, Beijing 100190, China; Email: whsun@iccas.ac.cn*
[c] *Faculty of Chemistry, University of Opole, Oleska 48, 45-052 Opole, Poland.*

†Appendix A. Supplementary material: CCDC 1008608, 1008609 and 1008610 contain the supplementary crystallographic data for **L2, Fe1** and **Fe2**. These data can be obtained free of charge from the Cambridge Crystallographic Data Centre via www.ccdc.cam.ac.uk/data_request/cif.

1 (a) J. Ma, C. Feng, S. Wang, K.-Q. Zhao, W.-H. Sun, C. Redshaw and G. A. Solan, *Inorg. Chem. Front.*, 2014, **1**, 14; (b) W. Zhang, W.-H. Sun and C. Redshaw, *Dalton Trans*., 2013, **42**, 8988; (c) T. Xiao, W. Zhang, J. Lai and W.-H. Sun, *C. R. Chim.*, 2011, **14**, 851; (d) C. Bianchini, G. Giambastiani, L. Luconi and A. Meli, *Coord. Chem. Rev.*, 2010, **254**, 431; (e) W.-H. Sun, S. Zhang and W. Zuo, *C. R. Chim.*, 2008, **11**, 307; (f) S. Jie, W.-H. Sun and T. Xiao, *Chin. J. Polym. Sci.*, 2010, **28**, 299; (g) R. Gao, W.-H. Sun and C. Redshaw, *Catal. Sci. Technol.*, 2013, **3**, 1172.

2 (a) W. -H. Sun, S. Song, B. Li, C. Redshaw, X. Hao, Y. Li and F. Wang, *Dalton Trans.*, 2012, **41**, 11999; (b) D. Jia, W. Zhang, W. Liu, L. Wang, W.-H. Sun and C. Redshaw, *Catal. Sci. Technol.*, 2013, **3**, 2737; (c) S. Kong, K. Song, T. Liang, C. Guo, W. -H. Sun, and C. Redshaw, *Dalton Trans.*, 2013, **42**, 9176; (d) S. Kong, C. Guo, W. Yang, L. Wang, W. -H. Sun and R. Glaser, *J. Organomet. Chem.*, 2013, **725**, 37; (e) Q. Liu, W. Zhang, D. Jia, X. Hao, C. Redshaw and W. -H. Sun, *Applied Catalysis A: General*, 2014, **475**, 195; (f) Q. Xing, K. Song, T. Liang, Q. Liu, W. -H. Sun and C. Redshaw, *Dalton Trans.*, 2014, **43**, 7830; (g) E. Yue, L. Zhang, Q. Xing, X. Cao, X. Hao, C. Redshaw and W. -H. Sun, *Dalton Trans.*, 2014, **43**, 423; (h) E. Yue, L. Zhang, Q. Xing, Q. Shi, X. Cao, L. Wang, C. Redshaw and W. -H. Sun, *Dalton Trans.*, 2014, **43**, 3339.

3 (a) B. L. Small, M. Brookhart and A. M. A. Bennett, *J. Am. Chem. Soc.*, 1998, **120**, 4049; (b) G. J. P. Britovsek, V. C. Gibson, B. S. Kimberley, P. J. Maddox, S. J. McTavish, G. A. Solan, A. J. P. White and D. J. Williams, *Chem. Commun.*, 1998, 849; (c) W. -H. Sun, W. Zhao, J. Yu, W. Zhang, X. Hao and C. Redshaw, *Macromol. Chem. Phys.*, 2012, **213**, 1266; (d) Q. Xing, T. Zhao, Y. Qiao, L. Wang, C. Redshaw and W. -H. Sun, *RSC Adv.*, 2013, **3**, 26184; (e) Q. Xing, T. Zhao, S. Du, W. Yang, T. Liang, C. Redshaw and W. -H. Sun, *Organometallics*, 2014, **33**, 1382**.**

4 (a) G. J. P. Britovsek, M. Bruce, V. C. Gibson, B. S. Kimberley, P. J. Maddox, S. Mastroianni, S. J. McTavish, C. Redshaw, G. A. Solan, S. Strömberg, A. J. P. White and D. J. Williams, *J. Am. Chem. Soc.*, 1999, **121**, 8728; (b) G. J. P. Britovsek, V. C. Gibson, B. S. Kimberley, S. Mastroianni, C. Redshaw, G. A. Solan, A. J. P. White and D. J. Williams, *Dalton Trans.*, 2001, 1639; (c) G. J. P. Britovsek, V. C. Gibson, S. Mastroianni, D. C. H. Oakes, C. Redshaw, G. A. Solan, A. J. P. White and D. J. Williams, *Eur. J. Inorg. Chem.*, 2001, 431; (d) G. J. P. Britovsek, V. C. Gibson, S. K. Spitzmesser, K. P. Tellmann, A. J. P. White and D. J. Williams, *Dalton Trans.*, 2002, 1159; (e) G. J. P. Britovsek, V. C. Gibson, O. D. Hoarau, S. K. Spitzmesser, A. J. P. White and D. J. Williams, *Inorg. Chem.*, 2003, **42**, 3454; (f) J. Yu, H. Liu, W. Zhang, X. Hao and W.-H. Sun, *Chem. Commun.*, 2011, **47**, 3257; (g) J. Lai, W. Zhao, W. Yang, C. Redshaw, T. Liang, Y. Liu and W. -H. Sun, *Polym. Chem.*, 2012, **3**, 787; (h) X. Cao, F. He, W. Zhao, Z. Cai, X. Hao, T. Shiono, C. Redshaw and W. -H. Sun, *Polymer*, 2012, **53**, 1870; (i) S. Wang, B. Li, T. Liang, C. Redshaw, Y. Li and W.-H. Sun, *Dalton Trans.*, 2013, **42**, 9188; (j) S. Wang, W. Zhao, X. Hao, B. Li, C. Redshaw, Y. Li and W.-H. Sun, *J. Organomet. Chem.*, 2013, **731**, 78.

5 (a) G. J. P. Britovsek, G. K. B. Clentsmith, V. C. Gibson, D. M. L. Goodgame, S. J. McTavish and Q. A. Pankhurst, *Catal. Commun.*, 2002, **3**, 207; (b) K. P. Bryliakov, N. V. Semikolenova, V. A. Zakharov and E. P. Talsi, *Organometallics*, 2004**,** **23**, 5375; (c) K. P. Bryliakov, N. V. Semikolenova, V. N. Zudin, V. A. Zakharov and E. P. Talsi, *Catal. Commun.*, 2004, **5**, 45; (d) V. L. Cruz, J. Ramos, J. S. Martínez, S. O. Gutiérrez and A. L. Toro, *Organometallics*, 2009, **28**, 5889; (e) R. Raucoules, T. Bruin, P. Raybaud and C. Adamo, *Organometallics*, 2009, **28**, 5358; (f) A. M. Tondreau, C. Milsmann, A. D. Patrick, H. M. Hoyt, E. Lobkovsky, K. Wieghardt and P. J. Chirik, *J. Am. Chem. Soc.*, 2010, **132**, 15046.

6 R. Raucoules, T. Bruin, P. Raybaud and C. Adamo, *Organometallics*, 2009, **28**, 5358.

7 (a) W.-H. Sun, S. Jie, S. Zhang, W. Zhang, Y. Song and H. Ma, *Organometallics*, 2006, **25**, 666; (b) S. Jie, S. Zhang, W.-H. Sun, X. Kuang, T. Liu and J. Guo, *J. Mol. Catal. A Chem.*, 2007, **269**, 85; (c) S. Jie, S. Zhang, K. Wedeking, W. Zhang, H. Ma, X. Lu, Y. Deng and W.-H. Sun, *C. R. Chim.*, 2006, **9**, 1500; (d) S. Jie,; S. Zhang and W.-H. Sun, *Eur. J. Inorg. Chem.*, 2007, 5584; (e) L. Wang, W.-H. Sun, L. Han, H. Yang, Y. Hu and X. Jin, *J. Organomet. Chem.*, 2002, **658**, 62.

8 M. Zhang, P. Hao, W. Zuo, S. Jie and W.-H. Sun, *J. Organomet. Chem.*, 2008, **693**, 483.

9 A. Boudier, P.-A. R. Breuil, L. Magna, C. Rangheard, J. Ponthus, H. Bourbigou and P. Braunstein, *Organometallics*, 2011, **30**, 2640.

10 (a) W.-H. Sun, P. Hao, S. Zhang, Q. Shi, W. Zuo, X. Tang and X. Lu, *Organometallics*, 2007, **26**, 2720; (b) Y. Chen, P. Hao, W. Zuo, K. Gao and W.-H. Sun, *J. Organomet. Chem.*, 2008, **693**, 1829; (c) L. Xiao, R. Gao, M. Zhang, Y. Li, X. Cao and W.-H. Sun, *Organometallics*, 2009, **28**, 2225.

11 (a) R. Gao, K. Wang, Y. Li, F. Wang, W.-H. Sun, C. Redshaw and M. Bochmann, *J. Mol. Catal. A: Chem.*, 2009, **309**, 166; (b) R. Gao, Y. Li, F. Wang, W.-H. Sun and M. Bochmann, *Eur. J. Inorg. Chem.*, 2009, **27**, 4149.

12 S. Song, R. Gao, M. Zhang, Y. Li, F. Wang and W.-H. Sun, *Inorg. Chim. Acta*., 2011, **376**, 373.

13 W.-H. Sun, P. Hao, G. Li, S. Zhang, W. Wang, J. Yi, M. Asma and N. Tang, *J. Organomet. Chem.*, 2007, **692**, 4506.

14 (a) S. Zhang, I. Vystorop, Z. Tang and W.-H. Sun, *Organometallics*, 2007, **26**, 2456; (b) S. Zhang, W.-H. Sun, X. Kuang, I. Vystorop and J. Yi, *J. Organomet. Chem.*, 2007, **692**, 5307; (c) S. Song, R. Gao, M. Zhang, Y. Li, F. Wang and W.-H. Sun, *Inorg. Chim. Acta*., 2011, **376**, 373.

15 (a) W. Zhang, W. B. Chai, W. -H. Sun, X. Q. Hu and C. Redshaw *Organometallics*, 2012, **31**, 5039; (b) W. -H. Sun, S. L. Kong, W. B. Chai, S. Takeshi, C. Redshawe and X. Q. Hu, *Applied Catalysis A: General*, 2012, **447**, 67.

16 V. K. Appukuttan, Y. Liu, B.C. Son, C.-S. Ha, H. Suh and II. Kim, *Organometallics*, 2011, **30**, 2285.

17 X. Xie, H. Huang, W. Mo, X. Fan, Z. Shen, N. Sun, B. Hu and X. Hu, *Tetrahedron: Asymmetry*, 2009, **20**, 1425.

18 D. Milstein and J. K. Stille, *J. Am. Chem. Soc.*, 1978, **100**, 3636.

19 (a) D. Guo, L. Han, T. Zhang, W.-H. Sun, T. Li and X. Yang, *Macromol. Theory. Simul.*, 2002, **11**, 1006; (b) D. Guo, X. Yang, T. Liu and Y. Hu, *Macromol. Theory Simul.*, 2001, **10**, 75; (c) D. Guo, X. Yang, L. Yang, Y. Li, T. Liu, H. Hong and Y. Hu, *J Polym Sci Part A:Polym Chem*, 2000, **38**, 2232.

20 (a) J. Yu, Y. Zeng, W. Huang, X. Hao and W.-H. Sun, *Dalton Trans.*, 2011, **40**, 8436; (b) L. Guo, H. Gao, L. Zhang, F. Zhu and Q. Wu, *Organometallics*, 2010, **29**, 2118.

21 G. M. Sheldrick, SHELXTL-97, Program for the Refinement of Crystal Structures; University of Gottingen: Germany, 1997.

22 L. Spek, *Acta Crystallogr., Sect. D: Biol. Crystallogr.,* 2009, **65**, 148.

23 A. D. Becke, *Phys. Rev. A*, 1988, **38**, 3098.

24 J. P. Perdew, *Phys. Rev. B*, 1986, **33**, 8822.

25 S. H. Vosko, L. Wilk and M. Nusair, *Can. J. Phys.*, 1980, **58**, 1200.

26 G. te Velde, F. M. Bickelhaupt, E. J. Baerends, C. F. Guerra, S. J. A. Gisbergen, J. G. Snijders and T. *J.* Ziegler, *Comput. Chem.*, 2001, **22,** 931.

27 C. F. Guerra, J. G. Snijders, G. te Velde and E. J. Baerends, *Theor. Chem. Acc.*, 1998, **99**, 391.

28 ADF 2013, SCM, Theoretical Chemistry, Vrije Universiteit, Amsterdam, The Netherlands, http://www.scm.com.

Graphical Abstract

for

2-(1-Aryliminoethyl)-9-arylimino-5,6,7,8-tetrahydrocycloheptapyridyl iron(II) dichloride: Synthesis, characterization, and the highly active and tunable active species in ethylene polymerization

Fang Huang, Qifeng Xing, Tongling Liang, Zygmunt Flisak, Bin Ye, Xinquan Hu, Wenhong Yang, Wen-Hua Sun

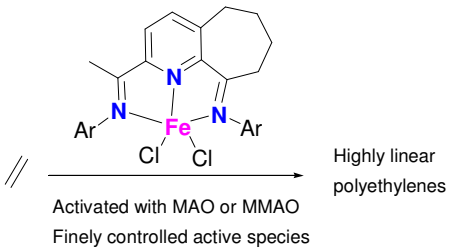

The 2-(1-Aryliminoethyl)-9-arylimino-5,6,7,8-tetrahydrocycloheptapyridyl iron(II) chloride complexes, activated by MAO or MMAO, showed high activities towards ethylene polymerization with producing linear polyethylenes.